Spatio-Temporal Evaluation of Physicochemical Parameters, Heavy Metals, and Pesticides in the Little Zab River

Mamoon Q. Salih^{1†}, Tara F. Tahir² and Wali M. Hamad²

¹Department of Chemistry, Faculty of Sciences and Health, Koya University, Koya, Kurdistan Region 44023, Iraq

²Department of Medical Microbiology, Faculty of Science and Health, Koya University, Koya, Kurdistan Region 44023, Iraq

Abstract—Water quality is a fundamental determinant of human health, influencing the prevalence of waterborne diseases and the overall safety of potable water. Contaminated water sources expose populations to microbial pathogens and toxic chemical contaminants, presenting significant public health and environmental challenges. In this study, a comprehensive assessment of water quality was conducted on a segment of the Little Zab River, situated in the Kurdistan region of Iraq. Water samples were meticulously collected from five strategically selected sites along the river, spanning across all four seasons, to evaluate temporal variations in water quality. In situ measurements of critical physico-chemical parameters, including pH, electrical conductivity, total dissolved solids, salinity, dissolved oxygen, density, and turbidity, were performed to establish baseline water quality profiles. Concurrently, laboratory analyses were performed to quantify the concentrations of selected heavy metals (mercury, cadmium, arsenic, zinc, iron, lead, and copper) and pesticides (α-cypermethrin, acetamiprid, dichloro-diphenyl-trichloroethane, and p,p'-DDD) using standardized methods. Descriptive statistical analyses, conducted using Excel and Statistical Package for Social Sciences, revealed significant spatial and seasonal fluctuations in both the physicochemical parameters and contaminant levels, with certain sites exhibiting concentrations that raise potential health and ecological concerns. The findings underscore the critical need for continuous monitoring of water used in agriculture and the implementation of targeted management strategies to mitigate contamination and protect public health in the region. This work contributes valuable insights into the interplay between natural processes and anthropogenic impacts on riverine water quality in arid and semi-arid environments.

Index Terms—Heavy metals, Little Zab River, Pesticides, Physicochemical, Water.

ARO-The Scientific Journal of Koya University Vol. XIV, No. 2 (2025), Article ID: ARO.12364. 15 pages DOI: 10.14500/aro.12364

Received: 20 June 2025; Accepted: 08 October 2025 Regular research paper; Published: 11 November 2025

ARO p-ISSN: 2410-9355, e-ISSN: 2307-549X

†Corresponding author's e-mail: mamoon.qader@koyauniversity.org Copyright © 2025 Mamoon Q. Salih, Tara F. Tahir and Wali M. Hamad. This is an open access article distributed under the Creative Composition License

(CC BY-NC-SA 4.0).

I. Introduction

In the last few decades, the expansion of cities and industry, as well as the intensification of agriculture, has resulted in massive pollution of freshwater systems with a huge number of chemical compounds industrially produced and naturally occurring. Although their concentrations are generally low, these pollutants are of major toxicological concern, as they are part of complex mixtures. Pollution of our natural water resources by a diverse range of pollutants is the most pivotal challenge posing a threat to the environment today on a global scale and is the result of accelerated urbanization, industrial expansion, and agricultural practices suburbs (Schwarzenbach, et al., 2006).

The influence of these activities on aquatic systems has been significant, with far-reaching public health concerns globally. Pollutants released into natural bodies of water have caused a drastic change in their chemical composition, frequently rendering them unfit for human consumption (Madhav, et al., 2020). The UN World Water Development Report 2024 states that the world's water crisis is getting worse under the combined impact of climate change and uncontrolled population growth. At the same time, insufficient access to safe drinking water and lack of environmental sanitation continue to be responsible for gastrointestinal diseases, nutrient malabsorption, and malnutrition, with children as the most at risk. The urgency of these challenges underscores the crucial need for innovative and integrated water solutions – and for investment in water infrastructure – in shaping a future that is both sustainable and equitable for all (Wu, 2020).

Rivers remain one of the most important sources of water for domestic, agricultural, and industrial uses in many regions, including the Kurdistan Region of Iraq. As a major regional tributary, the Little Zab River (LZR) is increasingly threatened by pollution from various sources, further endangering its water quality and ecosystem (Al-Dabbas, 2024; Kareem, et al., 2020).

Among these, heavy metals mercury (Hg), cadmium (Cd), arsenic (As), zinc (Zn), iron (Fe), lead (Pb), and copper (Cu) have specific biochemical properties that pose a risk to our

health owing to their durability, tendency to bio accumulate, and detrimental effects ([30, 31, 32, 33, 34]). Meanwhile, the release of pesticide residues, such as α-cypermethrin, acetamiprid, DDT, and p,p'-DDD into water environments through agricultural practices (Fig. 1) (Wu, et al., 2016). Some of these pesticides, still in use despite known ecological risks associated with their continued use, are well-known for their persistent nature and endocrine-disruptive potential on aquatic organisms and humans (Martyniuk, Mehinto, and Denslow, 2020).

Numerous studies have highlighted the importance of monitoring water quality through a comprehensive evaluation of physicochemical parameters and contaminant levels (Altenburger, et al., 2019; Hamadamin, et al., 2018; Olsen, Chappell and Loftis, 2012; Peluso, et al., 2021; Thakur and Devi, 2024). Many existing studies have focused narrowly on modest periods of sampling or particular contaminants, leaving gaps in our overall understanding of water quality over time. There is a clear need for more comprehensive assessments that span whole years and take into account both physical and chemical parameters alongside the major pollutants affecting the water. Addressing this gap, our study adopted a seasonal approach to explore the condition of a vital portion of the LZR in Iraqi Kurdistan. The LZR plays a pivotal role in supplying water for domestic use, agriculture, and industry; however, it unfortunately faces mounting pollution from diverse sources. This escalating contamination poses a serious threat to the water quality and the well-being of the surrounding ecosystem (Al-Dabbas, 2024).

In this study, water samples were collected at five carefully selected sites along the LZR and analyzed throughout all four seasons. We checked important water quality factors, including pH, electrical conductivity (EC), total dissolved solids (TDS), salinity, dissolved oxygen (DO), density, and turbidity, right at the sites to see how the water quality changed with the seasons. To fill critical gaps in existing research, we also quantified significant contaminants using reliable and validated laboratory methods. The procedure included analyzing heavy metals such as mercury (Valko, Morris and Cronin, 2005), Cd (Schoeters, et al., 2006), arsenic (Kaur, et al., 2024), zinc (Katimba, et al., 2024), iron (Sun, et al., 2008), lead (Koh, et al., 2015), and copper

Fig. 1. The structures of (a) dichloro-diphenyl-trichloroethane (DDT), (b) acetamiprid, (c) p,p'-DDD, and (d) alpha-cypermethrin.

(Kumar, et al., 2021), given their persistence, bioaccumulation potential, and adverse effects on human health. Pesticide residues, including α-cypermethrin, acetamiprid, DDT, and p,p'-DDD, were also analyzed due to their known persistence and documented risks to aquatic life and human endocrine systems (Carvalho, 2017; Jayaraj, Megha and Sreedev, 2016; Lazarević-Pašti, et al., 2018). The objective of this study was to perform a comprehensive spatio-temporal assessment of water quality in the LZR. We hypothesized that pollutant concentrations would increase downstream as a result of agricultural runoff and dam regulation, and that seasonal variation in agricultural activity and hydrological conditions would significantly affect the levels of both heavy metals and pesticides.

II. METHODS

A. Study Area

The study area encompasses a 175.08-km stretch of the LZR River, which constitutes approximately 44% of its total 400-km length. Originating in the Iranian mountains, the river flows into Kurdistan near Qaladiza, traversing a landscape with diverse climates, uneven terrain, and varying human impacts. Shaped by both natural forces and human activities such as urbanization, agriculture, and dam regulation, this area presents a unique opportunity to examine the interplay between physical and chemical factors, heavy metals, and pesticides in surface water. Five key sampling stations were established to assess spatial variations in water quality, with the river's terrain influencing flow characteristics (Fig. 2). Downstream, increased agricultural and industrial activities introduce additional contaminants, altering the river's composition.

B. Inlet of Kurdistan (Upstream)

This location, where the LZR first enters the Kurdistan region, is the primary source of water for the Dukan dam. Sampling at this location provides baseline water quality data before major human activities (e.g., agriculture, urbanization) or changes related to the reservoir (e.g., sedimentation, flow regulation) occur. This location is referred to as sample point 1 (SP1).

Dam inlet (darband)

The river stretches 47.7 km from Darband to the Dukan Dam reservoir. This section illustrates the impact of increased human activities (e.g., irrigation, livestock farming) and agricultural runoff on water quality degradation. The inlet near the town of Rayna represents the meeting point of tributaries feeding the reservoir, blending both upstream human and natural impacts. This location is referred to as sample point 2 (SP2).

Dam reservoir (convergence zone)

This sampling site, located in the stratified zones of the reservoir, reflects hydrological and seasonal changes. The tributaries contribute in different ways - winter and spring flows are primarily driven by snowmelt and rainfall, while summer and fall flows are often dominated by their smaller branches. This mixing zone results in sediment and nutrient

retention, as water from the LZR and other tributaries mixes. This site is designated Sample Point 3 (SP3).

Outlet of dukan dam (discharge)

Downstream from the controlled outflow, the waterway winds for approximately 75.85 km before merging with the Tigris River. This position is pivotal for assessing the consequences of reservoir management tactics, such as thermal layering and regulated outputs, on water quality, as it demonstrates the combined impacts of internal reservoir transformations alongside external human interventions. Referred to as Specimen Point 4, this site collects and combines variations in condition resulting from natural dynamics within the artificial body, as well as deliberate human adjustments made on its release.

End of research area (tagtag)

The Taqtaq confluence zone represents the downstream limit of the study area, integrating the combined contributions from upstream. The water quality of its tributaries is affected by discharges and pollution loads from agricultural, grazing, and fishing activities, as well as by discharges originating from dams or weirs built on its tributaries. The site, SP5, is a longitudinal integrative area of the whole monitored reach (end line).

In combination, the existing sampling network provides a consistent framework for the spatial resolution of pollutant distributions and identification of the hydrologic and anthropogenic controls on the water quality characteristics of the LZR.

C. Water Sampling and Preparation

Five sites were sampled along the LZR from headwaters to the last point before confluence, once per season to capture hydrological and agricultural variability. At each site, ~500 mL grab samples were collected 10-70 cm below the surface using pre-cleaned containers of materials appropriate to the analyte (polyethylene and glass). Containers were prerinsed with site water, and each bottle carried an indelible label with a unique ID, site coordinates, date/time, sampler name, and full preservation/storage details to ensure traceability. During transport, all samples were kept in insulated coolers maintained at 4°C. On receipt, preservation and storage followed international guidance: For heavymetal determinations, samples were pre-screened where necessary to remove particulates >100 μm and acidified with nitric acid to pH <2 to stabilize dissolved ions; acidified metal samples were stored in the dark at $\leq -18^{\circ}$ C, with permissible holding times of 1-6 months depending on the target element and downstream preparation. For pesticide determinations, samples were collected in dark (amber) glass to limit photolysis, transported cold as above, and transferred on the day of collection to ≤-18°C dark storage with a maximum holding time of 1 month before extraction; extraction and purification steps are provided in the dedicated "Pesticide Extraction and Cleanup" subsection and follow ISO guidance (solvent extraction and sorbent-based cleanup) so that the full procedure is explicit and reproducible. Field physicochemical parameters (pH, EC, temperature,

DO, turbidity, TDS/TSS, salinity, density) were measured on site whenever feasible; when short holding was unavoidable, samples were kept dark and cold and analyzed within 1 day. All work was conducted under ISO 5667 5667–1:2023 and American Public Health Association (APHA) guidelines (American Public Health Association, 2017).

D. Physicochemical Analysis

The water quality's physicochemical parameters were analyzed using procedures approved by APHA (American Public Health Association, 2017). Field measurements of pH, EC, TDS, salinity, and DO were conducted using the Hach HQ2200 Portable Multi-meter. The pH was measured using a calibrated glass electrode. EC and TDS were determined using a conductivity sensor, while salinity was derived from conductivity readings using the meter's internal conversion settings. DO was measured using a luminescent DO probe. All sensors were calibrated with standard solutions before measurement, in accordance with the manufacturer's instructions and APHA guidelines.

E. Heavy Metal Analysis

Elemental analysis was conducted using inductively coupled plasma optical emission spectroscopy (ICP-OES), employing a Varian ICP-OES Vista Pro instrument and an atomic absorption spectrometer (Varian 220, Australia). Mercury (Hg) was measured using Vapor Generation Atomic Absorption Spectroscopy coupled with Inductively Coupled Plasma Optical Emission Spectrometry (VGA-ICP-OES). As, Pb, and Cd were determined using graphite furnace atomic absorption spectroscopy (GF-AAS). Fe, Cu, and Zn were analyzed using Inductively Coupled Plasma Optical Emission Spectrometry (ICP-OES). These methods were selected to ensure high sensitivity and accuracy in detecting trace metal concentrations in water samples using the Varian ICP-OES Vista Pro, Australia. Analytical precision and accuracy were ensured through calibration with certified reference materials and procedural blanks (Das, 2023). Table I provides a comprehensive list of heavy metal parameters analyzed in water samples, detailing their measurement units and the analytical methods applied.

F. Pesticide Analysis

The determination of pesticide residues in water was achieved through liquid-liquid extraction, followed by gas

 $TABLE\ I$ Detection limit (mg/L) and test methods for heavy metals analysis

Parameters	Detection limit	Test method
Hg	0.0005 mg/L	VGA-ICP-OES
As	$0.0080~\mathrm{mg/L}$	GF-AAS
Pb	$0.0050~\mathrm{mg/L}$	GF-AAS
Cd	0.0020 mg/L	GF-AAS
Fe	0.0200 mg/L	ICP-OES
Cu	0.0200 mg/L	ICP-OES
Zn	0.0200 mg/L	ICP-OES

ICP-OES: Inductively coupled plasma optical emission spectroscopy, GF-AAS: Graphite furnace atomic absorption spectroscopy, Hg: Mercury, As: Arsenic, Pb: Lead, Cd: Cadmium, Fe: Iron, Cu: Copper, Zn: Zinc

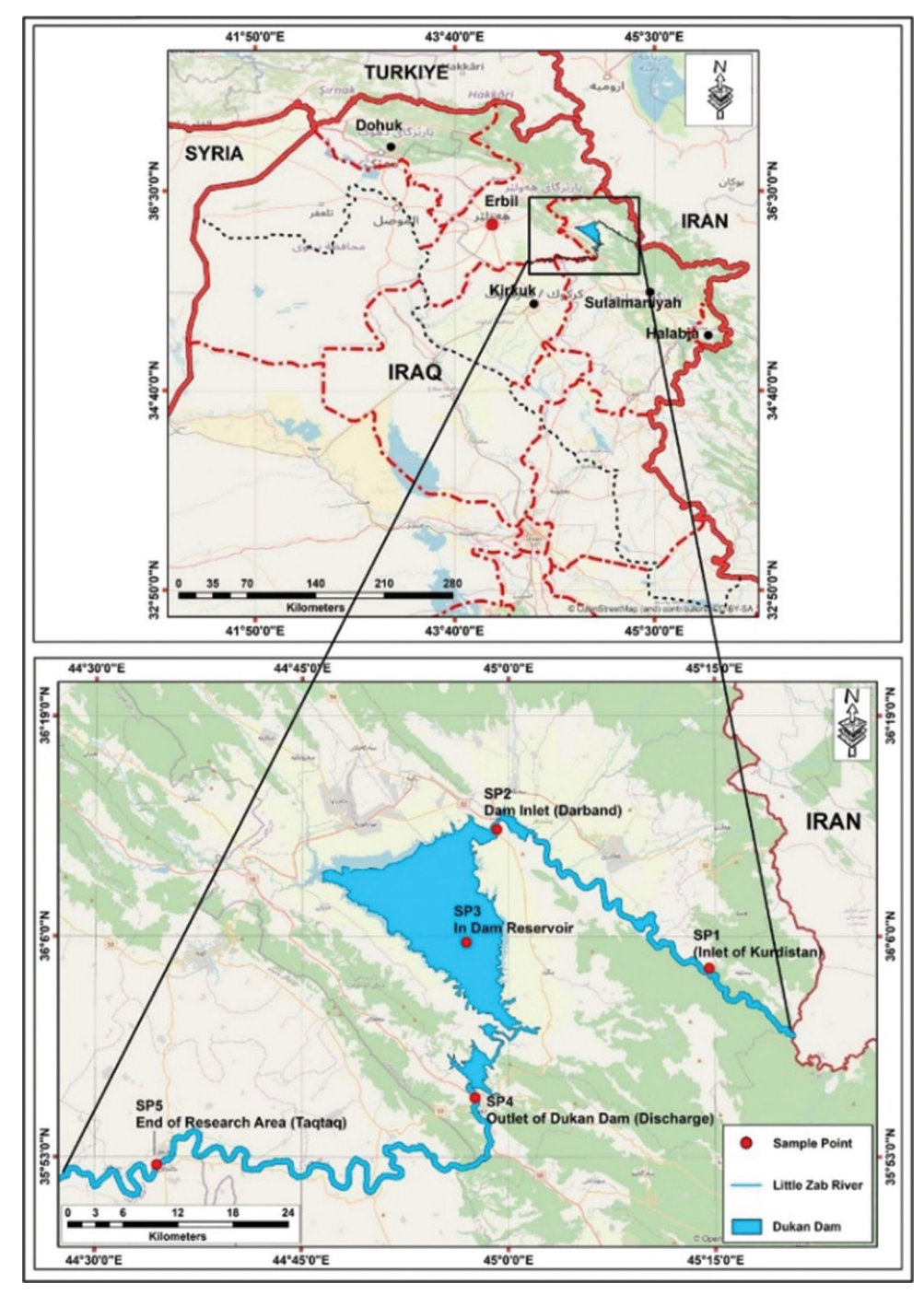


Fig. 2. Map of the study area and sample points created using ArcGIS version 10.8.

chromatography—mass spectrometry. Detection limit (mg/l) and test methods for pesticides analysis are shown in Table 2. This complex analysis was conducted *in situ*, adhering to standard procedures, using an inert carrier gas, helium, which facilitated the flow between the various components. The gas chromatograph was directly interfaced with the mass spectrometer, allowing for the extraction of samples containing a subset of nonpolar compounds with precision and accuracy. These samples were subsequently injected into the intricate gas chromatograph assembly. The mass spectrometer interface was maintained at an elevated yet regulated temperature of 280°C, and identification of target

analyses was enabled through the long-established process of electron ionization. Pesticide identities were confirmed and verified by comparing acquired spectra with reference databases. Thresholds of detection and measures of quality oversight were actualized according to renowned criteria to rigorously scrutinize generated results.

G. Data Interpretation and Statistical Analysis

Data interpretation in water analysis necessitates transforming collected information into meaningful insights. This convoluted process involves applying statistical and analytical techniques to identify trends, establish

connections, and detect patterns. Correct interpretation is indispensable for comprehending water quality readings and their repercussions, empowering informed decision-making, and assisting policy formation regarding water quality and protection (Therrien, Nicolaï and Vanrolleghem, 2020).

Stated in another way, however, this method employs mathematical and computational tools to probe the data sets for trends, relationships, and patterns. My research uses methods such as regression analysis, hypothesis testing, or correlation to conclude, consider significance judgments, and obtain reliable results (Schreiber, et al., 2022). In this class project, the Statistical Package for Social Sciences (SPSS) 19.0 (SPSS, Inc.), the software package for statisticians, was employed to assist students in further learn about making informed decisions and creating policy – and to let students know how a number of different aspects influence water quality indicators.

III. RESULTS AND DISCUSSION

A. Physicochemical Parameters and Assessment

Table III shows the physicochemical analysis which reveals a clear seasonal and spatial trends in parameters including pH, EC, TDS, salinity, DO, density, and turbidity (Prieto-Amparán, et al., 2018). The pH values ranged from 7.25 to 8.45, indicating slightly alkaline conditions. Statistical analysis confirms that pH values were significantly higher in spring (8.12), compared to summer, autumn, and winter, which all exhibited relatively stable but lower pH levels (\sim 7.33 to 7.38). Fig. 3a indicates that pH values are highest at the first inlet near the upstream, where transboundary influences prevail, and gradually decline to reach their minimum at the downstream confluence with the Tigris. Research shows that pH levels in aquatic systems vary seasonally and over time. This variability is largely driven by dynamic biogeochemical processes such as nitrification and CO, degassing, which influence proton cycling and acid-base equilibria (Hofmann, et al., 2009). Long-term data also reveal a seasonal decrease in pH that is mainly associated with lower freshwater discharge, and which changes the concentration of dissolved inorganic carbon, alkalinity, and biological activity (Ding, et al., 2019). Furthermore, decreases in precipitation due to climate change can lead to a rise in pH during the dry period, because reduced input of freshwater can lead to limited dilution, consequently increasing CO, degassing under stagnant hydrological conditions. These observed trends demonstrate the interaction between seasonal fluctuations, long-term hydrological changes, and climate conditions on pH fluctuations. Furthermore, this change can be considered to represent the transition between more or less fresh water entering the Kurdish region, and water that is more and more subjected to the effects of disturbing hydrological input, due to agricultural return flow waters, and urban waste waters.

The maximum values of EC and TDS were in spring, which were 326.2 μ S/cm and 242.0 ppm, respectively (p < 0.05), implying that runoff from the agricultural areas during early crop growth increased mineral contents of the

river water. Alike to other studies conducted in spring months in different locations showing similar trends of higher EC and TDS in spring with corresponding lower levels in later months (Al-Barwary, et al., 2018; Pokhrel and Rijal, 2020; Rawal, et al., 2024). A similar pattern is also observed in the current study. Summer, however, registered the lowest values of EC (232.5 μS/cm) and TDS (165.07 ppm), likely reflecting a dilution effect. EC is shown in Fig. 3b, which has a minimum value at the first sampling point and a maximum value at the downstream. Such a pattern corresponds to the expected accumulation of dissolved ions as the river receives runoff from major agricultural areas, urban wastewater, and diverse industrial releases at least at the dam inlet (Darband) and downstream section.

The trend for salinity was similar, with a maximum in spring (161.8 ppm) and minimum in summer (110.6 ppm). The seasonal variation in salinity is likely related to the weather, generating such seasonal variations in ion loading to the river due to precipitation and runoff. Besides these seasonal differences, Fig. 4a shows different spatial patterns of the five sampling points (Cayan and Peterson, 1993).

Seasonally low DO values in spring (0.21 mg/L) and autumn (0.23 mg/L) illustrated the seasonal variation of DO. Concentrations were higher in summer (0.26 mg/L) and winter (0.27 mg/L).

DO concentrations in water bodies are strongly influenced by seasonal temperature shifts and mixing dynamics. During winter and early spring, colder water holds more oxygen due to increased solubility, and the turnover of the water column during these seasons further distributes oxygen throughout the system (Li, Zou and Jiang, 2022). The increase of DO in summer could be related to enhance photosynthetic activity by aquatic plants and algae, as well as increased surface aeration driven by wind and biological mixing (Fig. 4b). The statistical analysis indicates a significant difference between winter/summer and spring/autumn, suggesting enhanced oxygen solubility at lower temperatures and possibly increased turbulence during colder months (Marcheva, et al., 2024).

Water density remained relatively stable across seasons, exhibiting minimal variation (ranging from 1.0020 to 1.0024 g/cm³), indicating that temperature-induced density fluctuations were not substantial enough to significantly influence stratification dynamics (Fig. 4c). Turbidity displayed significant seasonal fluctuations (Fig. 4d). It was highest in winter (15.77 NTU) and spring (13.11 NTU), while summer and autumn recorded much lower values (3.09 NTU and 2.87 NTU, respectively). The high winter turbidity suggests increased sediment resuspension due to rainfall and riverbed disturbances, whereas the lower summer values indicate relatively clear water conditions, possibly due to reduced runoff and sediment input (Lu, et al., 2023). In addition to these seasonal variations, the uploaded figure illustrates distinct spatial patterns across the five sampling points.

B. Heavy Metals Assessment

Heavy metal concentrations (Fe, Cu, Zn, Hg, As, Pb, and Cd) in the LZR are generally low, but both spatial and seasonal

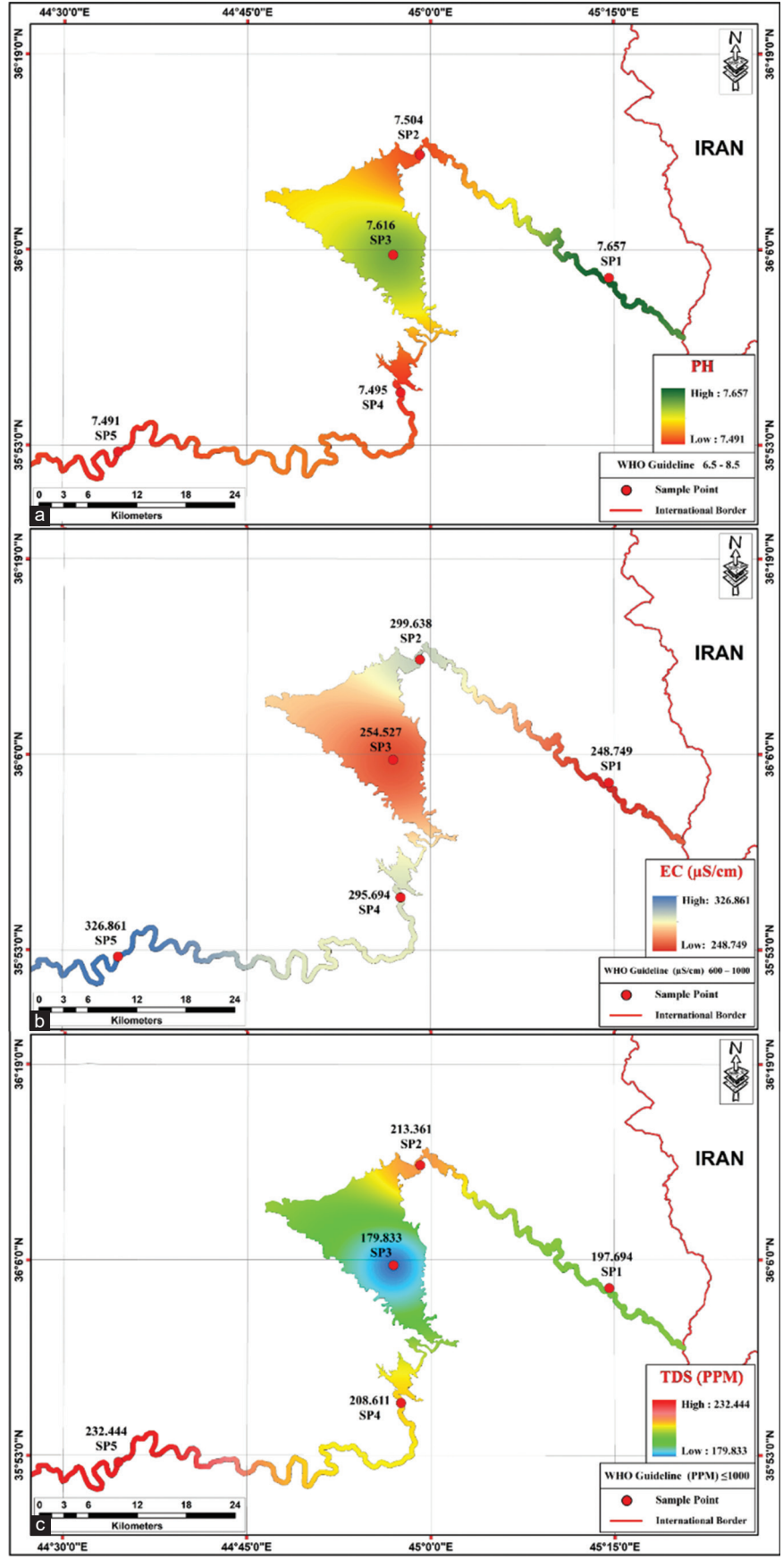


Fig. 3. Spatial distribution of (a) pH, (b) electrical conductivity (μ S/cm), and (c) total dissolved solids (ppm) across the study area.

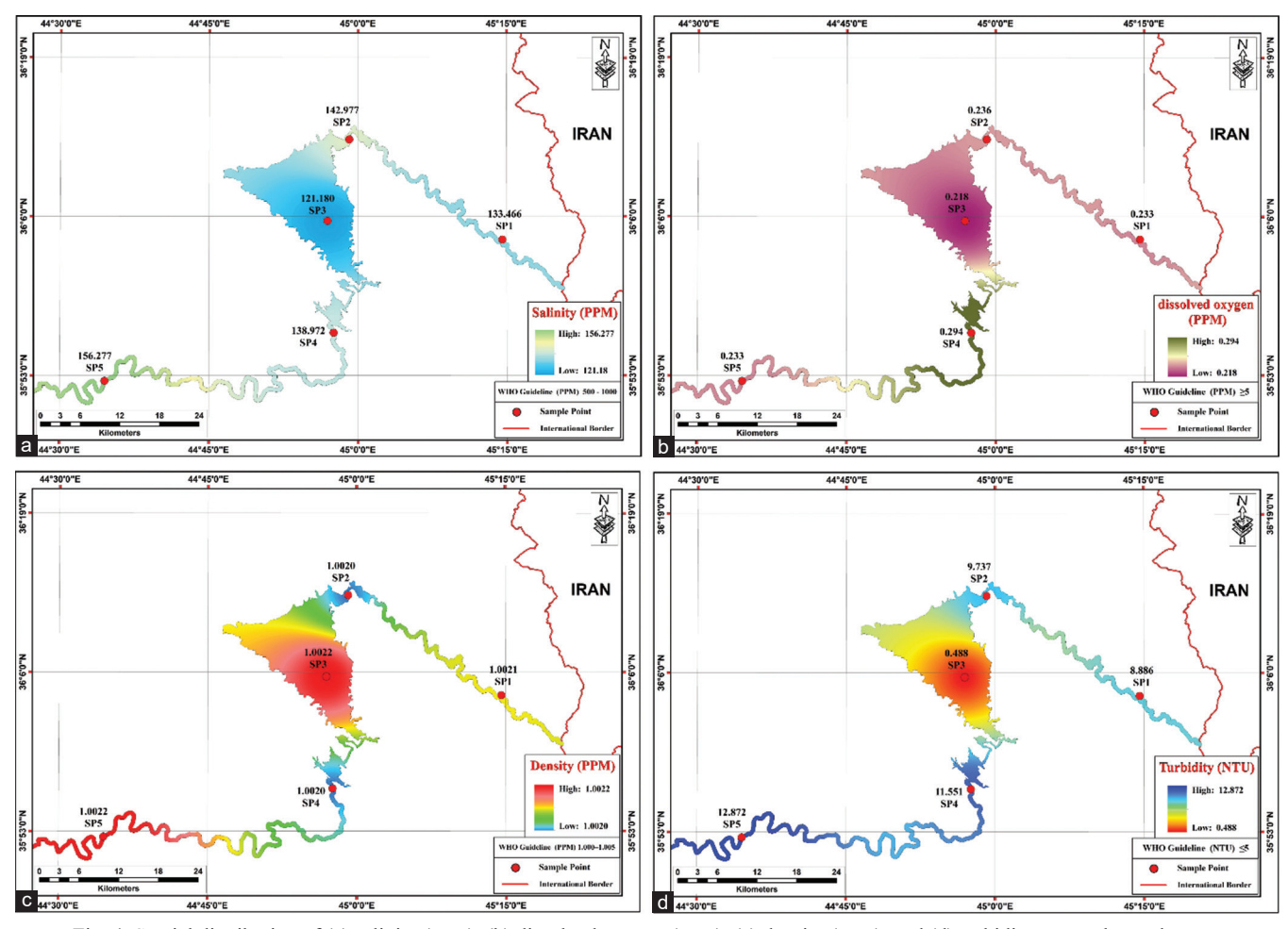


Fig. 4. Spatial distribution of (a) salinity (ppm), (b) dissolved oxygen (ppm), (c) density (ppm), and (d) turbidity across the study area.

variations are evident (Table V). The statistical analysis indicates that seasonal factors strongly influence metal levels, which reflects not only natural hydrological conditions but also varying anthropogenic inputs and sediment interactions.

In spring, the mean Fe concentration was approximately 0.21 mg/L, increasing progressively through summer (0.41 mg/L) and autumn (0.46 mg/L) to reach a significantly higher level in winter (0.97 mg/L). This pattern suggests that lower water flows and the potential remobilization of sediment-bound iron during winter contribute to elevated concentrations. The peak in iron concentration observed in winter is likely due to reduced water flow and increased interaction with bottom sediments, which may promote the release of sediment-bound iron (Hines, et al., 1984). Likewise, Zn concentrations were highly variable, with a low average of 1.70 mg/L in the spring, sharply increasing to around 5.56 mg/L in the summer of the same year, and then decreasing during the autumn (2.09 mg/L), and recorded an intermediate value in the winter (4.10 mg/L). This suggests that summer runoff, likely mixed with urban and agricultural inputs, may be responsible for the seasonal increase in zinc concentrations in the water (Shirasuna, et al., 2006).

Copper concentrations displayed a distinct seasonal pattern. The spring, autumn, and winter seasons had similar low concentrations, ranging from 0.16 to 0.19 mg/L. In contrast,

summer levels spiked to nearly 0.97 mg/L. Statistical tests (Tukey HSD, Table IV) corroborated that summer Cu concentration significantly differed from other seasons. This difference may be attributed to changes in industrial discharge patterns or shifts in water chemistry induced by higher temperatures during the summer months (Shirasuna, et al., 2006).

Fig. 5 illustrates the spatial distribution of iron, copper, and zinc concentrations across the five sampling points, revealing clear downstream enrichment patterns. For iron (Fig. 5a), the lowest concentrations were observed within the reservoir (SP3, 0.197 mg/L), while levels increased steadily toward the outlet (SP4, 0.214 mg/L) and peaked sharply at the downstream site SP5 (1.169 mg/L). This gradient reflects the influence of reduced dilution capacity, sediment remobilization, and cumulative pollutant inputs from tributaries and surrounding land uses. Copper (Fig. 5b) followed a similar pattern, with comparatively low values at SP3 (0.179 mg/L) and SP4 (0.19 mg/L), but higher concentrations both upstream (SP1 and SP2: 0.377-0.382 mg/L) and downstream (SP5: 0.742 mg/L). The indicates additional anthropogenic downstream peak contributions, likely from domestic and agricultural effluents, while upstream elevations may stem from agricultural runoff and transboundary inputs from Iran. Zinc (Fig. 5c) displayed

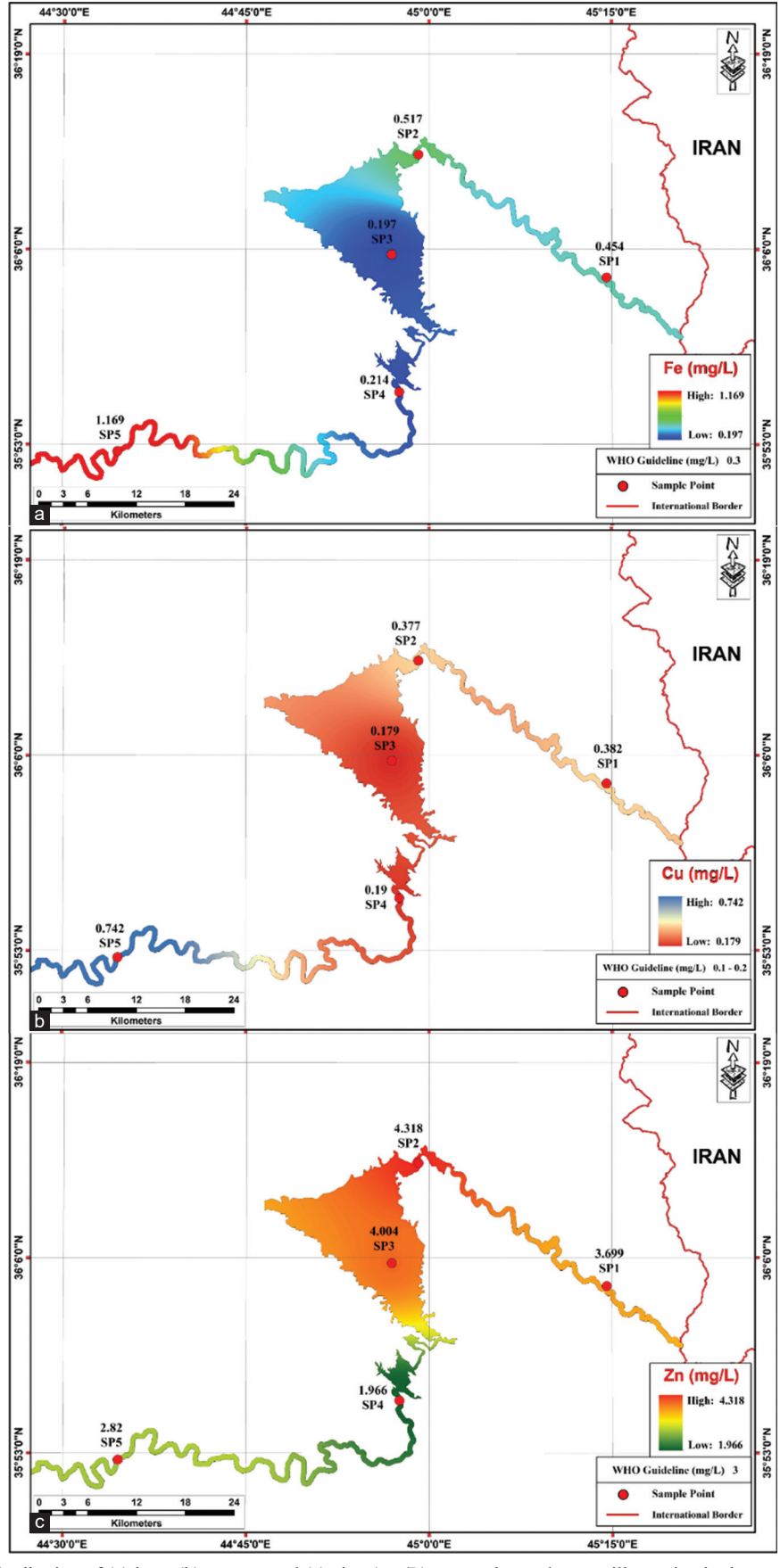


Fig. 5. Spatial distribution of (a) iron, (b) copper, and (c) zinc (mg/L) across the study area, illustrating both upstream agricultural influences (notably at sample point 2), reservoir-driven dilution and sediment interactions (sample point 3-sample point 4), and cumulative downstream contamination at sample point 5.

 $TABLE\ II$ Detection Limit (Mg/L) and Test Methods for Pesticides Analysis

Parameters	Detection limit (mg/L)	Test method
α-cypermethrin	0.0002	LLE-GC-MS
Acetamiprid	0.0010	LLE-GC-MS
DDT	0.0002	LLE-GC-MS
p, p'-DDD	0.0002	LLE-GC-MS

DDT: Dichloro-diphenyl-trichloroethane

Table III

Comparative analysis of the physicochemical attributes at 5 sample points during 4 seasons

	10	JINTS DOK	NG 4 SEAS	5115		
Season	Parameters	SP1	SP2	SP3	SP4	SP5
Spring	pН	8.45	8.14	8.2	7.87	7.96
	EC (µS/cm)	352	337	319	353	347
	TDS (ppm)	250	239	226	250	246
	Salinity (ppm)	169	161	152	169	166
	DO	0.2	0.2	0.25	0.25	0.15
	Density	1.0018	1.0018	1.002	1.0022	1.0023
	Turbidity	10.12	16.1	0.7	20.3	20.17
Summer	pН	7.39	7.25	7.44	7.3	7.49
	EC (µS/cm)	173.9	203	191	242	347
	TDS (ppm)	124	144	136	172	246
	Salinity (ppm)	83.8	97.2	91.5	115	165
	DO	0.3	0.25	0.25	0.3	0.25
	Density	1.002	1.0022	1.002	1.002	1.0025
	Turbidity	4.2	4	0.2	3.5	4
Autumn	pН	7.39	7.35	7.49	7.43	7.25
	EC (µS/cm)	313	374	294	297	282
	TDS (ppm)	222	266	209	211	200
	Salinity (ppm)	149	179	140	142	135
	DO	0.2	0.2	0.2	0.25	0.2
	Density	1.0026	1.0025	1.002	1.0023	1.0025
	Turbidity	2.5	2.6	0.2	2.45	2.5
Winter	pН	7.4	7.28	7.31	7.4	7.3
	EC (µS/cm)	269	282	211	289	329
	TDS (ppm)	191	201	149	202	233
	Salinity (ppm)	129	135	101	137	157
	DO	0.2	0.3	0.2	0.35	0.3
	Density	1.0025	1.0022	1.0018	1.0015	1.0019
	Turbidity	18.89	17.8	0.95	20.1	21.4

SP1: Sample point 1, SP2: Sample point 2, SP3: Sample point 3, SP4: Sample point 4, SP5: Sample point 5, EC: Electrical conductivity, TDS: Total dissolved solids, DO: Dissolved oxygen

 $TABLE\ IV \\ TUKEY\ HSD\ TEST\ RESULTS\ FOR\ HEAVY\ METALS\ IN\ THE\ LZR$

Metal	Season groupings (homogeneous subsets)	Significance (p)
Fe	Spring <summer=autumn<winter< td=""><td>0.025</td></summer=autumn<winter<>	0.025
Cu	Spring=Winter=Autumn <summer< td=""><td>1.000</td></summer<>	1.000
Zn	Spring <autumn=winter<summer< td=""><td>0.014</td></autumn=winter<summer<>	0.014
Hg	Summer <autumn<winter<spring< td=""><td>0.038</td></autumn<winter<spring<>	0.038
As	Spring=Winter <summer=autumn< td=""><td>0.470</td></summer=autumn<>	0.470
Pb	Winter <spring<autumn<summer< td=""><td>1.000</td></spring<autumn<summer<>	1.000
Cd	Winter <spring=summer<autumn< td=""><td>0.985</td></spring=summer<autumn<>	0.985

Hg: Mercury, As: Arsenic, Pb: Lead, Cd: Cadmium, Fe: Iron, Cu: Copper, Zn: Zinc

the most pronounced variability, with elevated concentrations at SP2 (4.318 mg/L) and SP3 (4.004 mg/L), followed by a decrease at the dam outlet (SP4, 1.966 mg/L) and another increase at SP5 (2.82 mg/L). This pattern suggests that agricultural runoff entering near SP2 substantially elevates

TABLE V Comparative analysis of some heavy metals attributes at 5 sample points during 4 seasons

DURING 4 SEASONS						
Season	Parameters	SP1	SP2	SP3	SP4	SP5
Spring	Fe (mg/L)	0.22	0.21	0.20	0.21	0.20
	Cu (mg/L)	0.19	0.17	0.15	0.20	0.11
	Zn (mg/L)	0.17	0.20	0.74	0.21	0.55
	Hg (mg/L)	0.00040	0.00043	0.00031	0.00179	0.00055
	As (mg/L)	0.0710	0.07247	0.07194	0.07	0.07317
	Pb (mg/L)	0.0510	0.05144	0.05244	0.054	0.055
	Cd (mg/L)	0.02167	0.021	0.02134	0.02	0.024
Summer	Fe (mg/L)	0.20	0.21	0.21	0.20	1.24
	Cu (mg/L)	1.01	0.94	0.19	0.25	2.47
	Zn (mg/L)	8.84	11.0	2.52	2.17	3.27
	Hg (mg/L)	0.00055	0.00056	0.00050	0.00058	0.00061
	As (mg/L)	0.07434	0.07601	0.07334	0.07402	0.07701
	Pb (mg/L)	0.05794	0.05684	0.0545	0.056	0.059
	Cd (mg/L)	0.01917	0.020	0.02367	0.02267	0.02347
Autumn	Fe (mg/L)	0.40	0.74	0.20	0.21	0.78
	Cu (mg/L)	0.22	0.21	0.20	0.16	0.20
	Zn (mg/L)	5.01	0.21	3.94	0.84	0.47
	Hg (mg/L)	0.00065	0.00067	0.00069	0.00060	0.00068
	As (mg/L)	0.07417	0.07827	0.0769	0.0712	0.079
	Pb (mg/L)	0.05467	0.05517	0.056	0.05417	0.056
	Cd (mg/L)	0.02684	0.02484	0.02594	0.025	0.027
Winter	Fe (mg/L)	1.0	0.94	0.19	0.25	2.47
	Cu (mg/L)	0.13	0.21	0.20	0.16	0.21
	Zn (mg/L)	0.80	5.87	2.17	4.67	7.01
	Hg (mg/L)	0.00072	0.00070	0.00072	0.00075	0.00079
	As (mg/L)	0.07154	0.073	0.07377	0.0714	0.07367
	Pb (mg/L)	0.04954	0.04867	0.049	0.0486	0.050
	Cd (mg/L)	0.01787	0.01847	0.01567	0.016	0.019

Hg: Mercury, As: Arsenic, Pb: Lead, Cd: Cadmium, Fe: Iron, Cu: Copper, Zn: Zinc

Zn levels, while reservoir mixing temporarily reduces concentrations at SP4 before downstream cumulative inputs drive levels higher again. Overall, the maps confirm that SP5 consistently receives the greatest pollutant burden, highlighting the role of cumulative downstream contamination from multiple sources, including agricultural runoff, urban wastewater, and dam-related sediment release.

Hg and As showed less pronounced seasonal variability, with Hg concentrations reaching their highest levels in spring (approximately 0.0014 mg/L) and then stabilized at lower levels (ranging between 0.56 and 0.0007 mg/L) during the subsequent seasons. Arsenic levels, though relatively stable (with means ranging from 0.0717 to 0.0759 mg/L), tended to be slightly elevated in summer and autumn compared to spring and winter. Pb displayed moderate seasonal fluctuations; its mean concentration ranged from about 0.0492 mg/L in winter to 0.0568 mg/L in summer. Finally, Cd demonstrated significant variability, with a mean of 0.0216 mg/L in spring, a slight increase in summer, peaking at 0.0259 mg/L in autumn, and then declining to 0.0174 mg/L in winter. The observed increase in Cd concentration during summer and autumn may be attributed to reduced river discharge and increased runoff from agricultural land and urban areas, where Cd from fertilizers, industrial waste, and untreated sewage can accumulate and enter the water. As Cd primarily exists as CdCO3 in river systems, seasonal lowflow conditions enhance its mobilization from sediments and

surrounding catchments (Kumar, et al., 2022; Rather, et al., 2022; Syers, et al., 1986).

The dam outlet (SP4) exhibited elevated concentrations of certain heavy metals (Figs. 5 and 6). This is consistent with expectations from dam management practices, where bottom discharge can mobilize pollutants accumulated in the reservoir's sediments. The dam reservoir (SP3) generally showed lower concentrations, suggesting that dilution processes within the reservoir may offset some of the input from tributaries. However, seasonal differences also emerged, for example, summer and autumn occasionally recorded slightly higher metal levels, likely reflecting the combined impacts of concentrated runoff during low-flow conditions and increased pollutant inputs from adjacent urban and agricultural activities (Park, et al., 2008). Overall, the data support the hypothesis that sample points receiving direct anthropogenic discharges (SP2 and SP5) are more vulnerable to heavy metal contamination, warranting focused monitoring efforts. These seasonal differences, supported by statistical significance tests, highlight that the river's heavy metal profile is not static but is dynamically influenced by seasonal hydrological conditions and variable anthropogenic pressures (Yao, et al., 2014).

Fig. 6 presents the spatial distribution and average concentrations of arsenic, Cd, mercury, and lead across the five sampling points of the LZR. Similar to the behavior observed for

Fe, Cu, and Zn (Fig. 5), the downstream site (SP5) consistently exhibited the highest concentrations of all four toxic metals. For instance, as ranged from 0.0716 mg/L at SP4 to 0.0757 mg/L at SP5, while Cd increased from 0.0209 mg/L at SP4 to 0.0234 mg/L at SP5. Pb also showed a marked rise at SP5 (0.0533 mg/L) compared with upstream sites (52.76 μ g/L at SP1). Hg displayed a more variable pattern, with the highest value recorded at SP1 (0.0148 mg/L), but concentrations remained elevated at SP2 and SP5 compared to intermediate sites.

The observed spatial patterns suggest that anthropogenic inputs in the downstream area, including agricultural runoff, untreated domestic wastewater, and industrial discharges, contribute significantly to metal contamination in this section of the river. The proximity of SP5 to major agricultural fields and small industrial units may explain its elevated concentrations. The elevated As levels across all sites are particularly concerning, as they consistently exceed the World Health Organization (WHO) permissible limit of 0.01 mg/L for drinking water. Likewise, Cd and Pb concentrations at all sampling points are well above guideline values, highlighting potential risks to both ecological and human health.

C. Pesticides Assessment

The pesticide analysis focused on α -cypermethrin, acetamiprid, DDT, and p,p'-DDD compounds, as they are

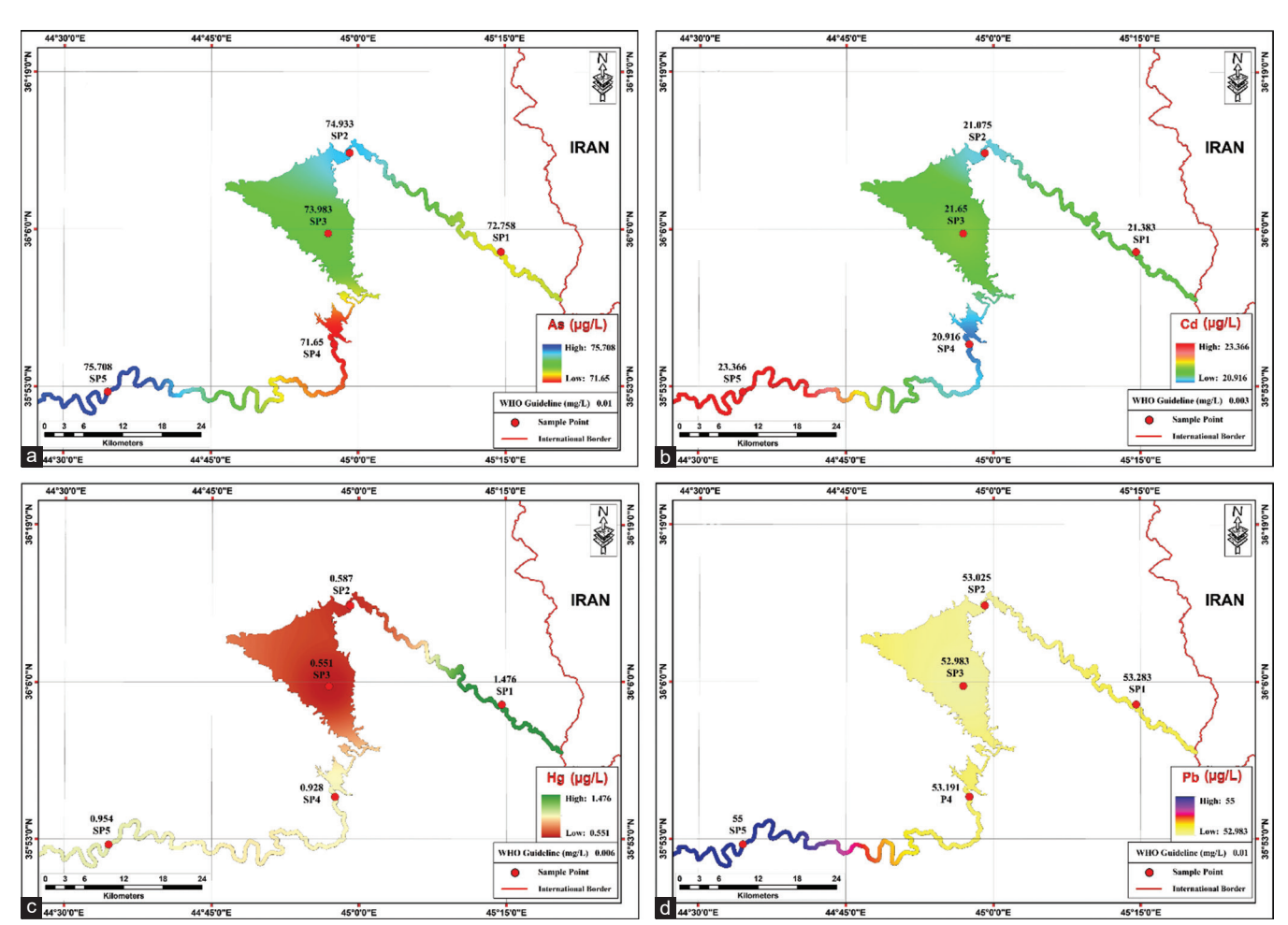


Fig. 6. Spatial distribution of (a) arsenic, (b) cadmium, (c) mercury, and (d) lead across the study area. Data show consistently elevated concentrations at the downstream site (sample point 5), indicating the influence of anthropogenic activities.

among the most commonly used pesticides in the region (Qasim, 2024). Table VI Comparative analysis of pesticides attributes at 5 sample points during 4 seasons. These pesticides were selected based on multiple criteria: (i) agricultural relevance, since α -cypermethrin (a pyrethroid) and acetamiprid (a neonicotinoid) are extensively applied in local farming practices for pest management on wheat, maize, and horticultural crops; (ii) environmental persistence, as organochlorines such as DDT and its degradation product p,p'-DDD remain in soils and sediments for decades despite restrictions, making them priority contaminants; and (iii) toxicological importance, given their known impacts on aquatic life, endocrine disruption in humans, and potential for bioaccumulation. In the spring season, pesticide concentrations were generally low across most sampling points, with α-cypermethrin values ranging from 0.0010 to 0.0011 mg/L at SP1, SP2, SP3, and SP5. Notably, SP4 (dam outlet) recorded a spike (0.0044 mg/L) for α-cypermethrin, suggesting that reservoir discharge may entrain higher loads of this compound. Acetamiprid during spring showed a modest increase toward SP5 (0.009 mg/L), whereas legacy pesticides such as DDT and p,p'-DDD maintained relatively uniform levels (approximately 0.0013-0.0019 mg/L and 0.0009-0.0011 mg/L, respectively) with a slight elevation at SP5. This pattern is consistent with the expectation that the dam outlet (SP4) and the downstream confluence (SP5) would reflect cumulative impacts of agricultural activities and urban effluents, as SP2 (Dam Inlet/Darband) is a known hotspot for direct runoff (Al-Dabbas, 2024).

In summer and autumn, acetamiprid levels exhibited a slight increase (0.009–0.010 mg/L) across all sampling points compared to the spring season. Meanwhile, α -cypermethrin and DDT levels were largely consistent with previous seasons. The marginally higher acetamiprid levels in autumn are consistent with seasonal pesticide application practices, where its use peaks following the summer growing season. The slightly higher p,p'-DDD values at SP5 (up to

TABLE VI

COMPARATIVE ANALYSIS OF PESTICIDES ATTRIBUTES AT 5 SAMPLE
POINTS DURING 4 SEASONS

Season	Parameters	SP1	SP2	SP3	SP4	SP5
Spring	α-cypermethrin (mg/L)	0.0011	0.0011	0.001	0.0044	0.0011
	Acetamiprid (mg/L)	0.006	0.005	0.008	0.008	0.009
	DDT (mg/L)	0.0015	0.0016	0.0017	0.0013	0.0019
	p, p'-DDD (mg/L)	0.001	0.001	0.0009	0.0011	0.001
Summer	α-cypermethrin (mg/L)	0.0013	0.0012	0.0013	0.0013	0.0013
	Acetamiprid (mg/L)	0.007	0.006	0.008	0.008	0.008
	DDT (mg/L)	0.0017	0.0018	0.0018	0.0019	0.002
	p, p'-DDD (mg/L)	0.0012	0.0012	0.0013	0.0012	0.0014
Autumn	α-cypermethrin (mg/L)	0.0013	0.0013	0.0013	0.0013	0.0014
	Acetamiprid (mg/L)	0.009	0.009	0.01	0.009	0.01
	DDT (mg/L)	0.0016	0.0016	0.0016	0.0015	0.0018
	p, p'-DDD (mg/L)	0.0013	0.0014	0.0014	0.0013	0.0014
Winter	α-cypermethrin (mg/L)	0.0013	0.0014	0.0014	0.0013	0.0014
	Acetamiprid (mg/L)	0.009	0.00825	0.008	0.009	0.0095
	DDT (mg/L)	0.0015	0.0017	0.0018	0.0018	0.0019
	p, p'-DDD (mg/L)	0.0012	0.0049	0.0012	0.0012	0.0013

DDT: Dichloro-diphenyl-trichloroethane

0.0014 mg/L) further indicate the cumulative impact of both current and historical pesticide inputs as the river flows downstream through agricultural zones (Lalín-Pousa, et al., 2025; Mermer, et al., 2020).

Statistical analysis revealed seasonal patterns in pesticide concentrations. The Tukey HSD test indicated no seasonal differences in α -cypermethrin (p = 0.742), suggesting that levels were consistent throughout the season. Conversely, acetamiprid was found at higher levels in autumn and winter than in spring and summer (p < 0.05). This pattern is likely due to the additional use of pesticides after the main growing season (Afzal, et al., 2024). DDT concentrations exhibited significant variation across different seasons (p = 0.017), with the highest mean values recorded during summer. This trend may be linked to the chemical's persistence and slower degradation in warmer temperatures. Meanwhile, p,p'-DDD did not exhibit statistically significant seasonal differences, indicating a consistent legacy residue pattern in the study area.

The study area, which spans from the upstream inflow near Kaladze to the confluence with the Tigris River, is subject to diverse anthropogenic pressures. SP1, serving as a transboundary reference point, displays baseline pesticide levels that likely include contributions from agricultural practices in Iran. In contrast, SP2, located at the Dam Inlet near Rayna, is exposed to intensive agricultural runoff, especially during periods of active pesticide application (e.g., the use of α -cypermethrin in spring and acetamiprid in autumn). The dam reservoir (SP3) appears to moderate pesticide concentrations through dilution, whereas SP4 (dam outlet) reveals the influence of reservoir management practices, potentially reintroducing concentrated pesticide residues into the downstream flow. Finally, the cumulative effects observed at SP5 corroborate the expectation that downstream areas receive compounded inputs from upstream activities, including both ongoing pesticide applications and historical residues such as DDT and p,p'-DDD.

Fig. 7 illustrates the spatial distribution of pesticide concentrations across the study area. Panel (a) maps α-cypermethrin levels, which ranged between 0.0011 and 0.0020 mg/L. Panel (b) shows acetamiprid concentrations, which varied between 0.0076 and 0.0090 mg/L. The spatial pattern reveals slightly elevated concentrations at SP3 and SP4 ($\sim 0.0084-0.0086$ mg/L), while the maximum value was detected at SP2 (0.0090 mg/L). SP1 and SP5 presented relatively lower levels (~0.0076–0.0090 mg/L), although still above the WHO guideline value, indicating the widespread presence of this pesticide across the basin. Panel (c) depicts the distribution of DDT. The concentrations remained low and fairly uniform across most sampling points (0.00157– 0.00167 mg/L), with slightly higher levels at SP2 and SP3 (0.00162-0.00167 mg/L). Although values are close, the consistent detection of DDT highlights its persistence as a legacy pollutant in the river ecosystem, likely due to past agricultural applications (Turusov, Rakitsky, and Tomatis, 2002). Panel (d) presents p,p'-DDD, a metabolite of DDT, with concentrations ranging between 0.00116 and 0.00208 mg/L. The highest concentration occurred at SP2 (0.00208 mg/L), followed by slightly elevated levels

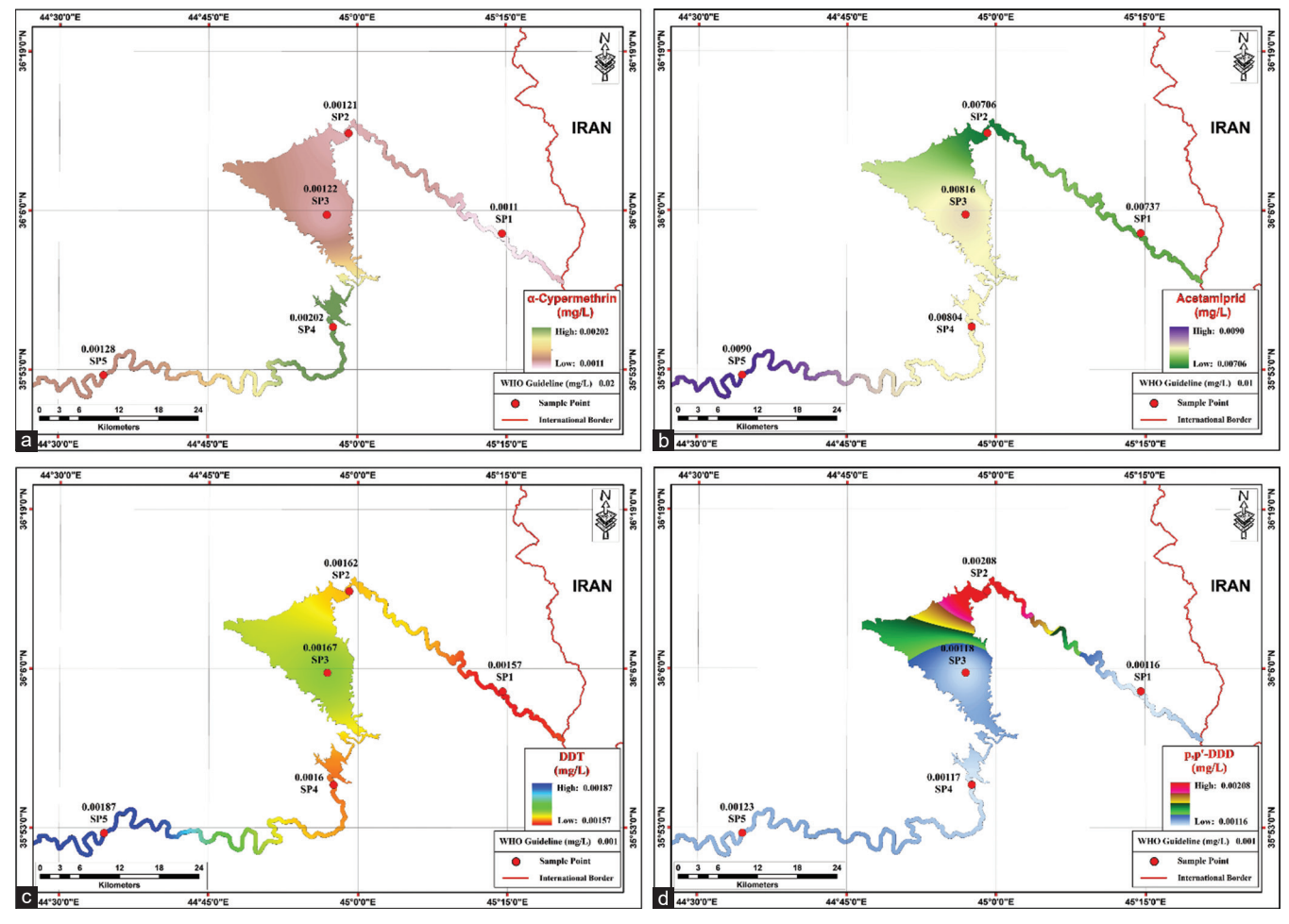


Fig. 7. Spatial distribution of pesticide concentrations across the Little Zab River: (a) α-cypermethrin, (b) acetamiprid, (c) dichloro-diphenyl-trichloroethane, and (d) p,p'-DDD (mg/L). Values represent average concentrations at each sampling point (sample point 1- sample point 5). Elevated levels at specific sites, particularly near the dam outlet (sample point 4) and agricultural zones (sample point 2- sample point 3).

at SP3 and SP4 (~0.0017–0.0018 mg/L). In contrast, SP1 and SP5 showed lower values (~0.00116–0.00123 mg/L). Together, these spatial patterns highlight both legacy and current pesticide contamination sources. Elevated pesticide levels near the dam (SP4) and agricultural zones (SP2 and SP3) point toward the combined impact of agricultural runoff, hydrological regulation, and historical pesticide use in shaping the contamination profile of the LZR.

D. Risk Assessment of Heavy Metals and Pesticides

To provide a more comprehensive evaluation of the potential hazards associated with detected pollutants, the concentrations of heavy metals (Fe, Cu, Zn, Hg, As, Pb, Cd) and pesticides (acetamiprid, DDT, and α-cypermethrin) were compared with the World Health Organization (WHO, 2017) drinking water quality guidelines. In addition, a Hazard Quotient (HQ) analysis was performed, where HQ was defined as the ratio between the measured concentration (C_measured) at each sampling point and the corresponding WHO guideline value (C_guideline). An HQ value >1 indicates potential human health or ecological risk, while HQ < 1 suggests limited concern.

The results of the HQ analysis are summarized in Table VII. Among the metals, arsenic, Cd, and lead

consistently exhibited HQ values well above 1 across all sites and seasons, ranging from 5.9 to 9.0 for Cd, 4.9 to 5.9 for Pb, and 7.0 to 7.8 for As. This indicates that these metals represent the most critical contaminants in the LZR and pose a significant potential risk to human health. Mercury occasionally exceeded guideline limits, with HQ values up to 0.67 in spring and 0.13 in winter, while copper and zinc generally remained below the risk threshold (HQ < 1). Iron, although an essential element, showed elevated HQ values at some downstream sites in winter (up to 8.2 at SP5), suggesting localized concern.

For pesticides, DDT and its derivative p,p'-DDD displayed HQ values between 1.3 and 2.0 across seasons, indicating potential ecological and human health risks due to their persistence and bioaccumulative nature. In contrast, acetamiprid and α-cypermethrin showed HQ values mostly below 0.2, indicating a lower immediate risk at the measured concentrations. Spatially, the highest HQ values were observed at downstream sites (SP4 and SP5). Seasonally, winter samples showed more pronounced risks, particularly for Fe, Pb, Cd, and As. These trends point to the influence of agricultural runoff, industrial effluents, and hydrological regulation on pollutant distribution.

TABLE VII

SEASONAL VARIATION OF HAZARD QUOTIENT (HQ) VALUES FOR HEAVY METALS

AND PESTICIDES ACROSS FIVE SAMPLING PO

INTS (SP1-SP5), CALCULATED WITH RESPECT TO WHO (2017) DRINKING

WATER QUALITY GUIDELINE VALUES. HQ>1 INDICATES POTENTIAL

ECOLOGICAL OR HUMAN HEALTH RISK

Season	Parameters	WHO value (mg/L)	SP1	SP2	SP3	SP4	SP5
Spring	Fe	0.3	0.733	0.7	0.667	0.7	0.667
	Cu	2.0	0.095	0.085	0.075	0.1	0.055
	Zn	3.0	0.057	0.067	2.467	0.067	0.183
	Hg	0.006	0.667	0.072	0.05	0.298	0.092
	As	0.01	7.1	7.247	7.194	7	7.317
	Pb	0.01	5.1	5.144	5.244	5.4	5.5
	Cd	0.003	7.223	7	7.113	6.667	8
	Acetamiprid	0.07	0.085	0.071	0.114	0.114	0.128
	DDT	0.001	1.5	1.6	1.7	1.3	1.9
	α-cypermethrin	0.02	0.055	0.055	0.05	0.22	0.055
Summer	Fe	0.3	0.667	0.667	0.667	0.667	4.133
	Cu	2.0	0.5	0.47	0.095	0.125	1.235
	Zn	3.0	2.947	3.667	0.84	0.723	1.09
	Hg	0.006	0.092	0.093	0.083	0.097	0.1
	As	0.01	7.434	7.6	7.334	7.4	7.7
	Pb	0.01	5.794	5.684	5.45	5.6	5.9
	Cd	0.003	6.39	6.667	7.89	7.557	7.823
	Acetamiprid	0.07	0.100	0.085	0.114	0.114	0.114
	DDT	0.001	1.7	1.8	1.8	1.9	2
	α -cypermethrin	0.02	0.065	0.06	0.065	0.065	0.065
Autumn	Fe	0.3	1.333	2.467	0.667	0.667	2.6
	Cu	2.0	0.11	0.105	0.1	0.08	0.1
	Zn	3.0	1.667	0.07	1.313	0.28	0.157
	Hg	0.006	0.108	0.112	0.115	0.1	0.113
	As	0.01	7.417	7.827	7.69	7.12	7.9
	Pb	0.01	5.467	5.517	5.6	5.417	5.6
	Cd	0.003	8.947	8.28	8.647	8.333	9
	Acetamiprid	0.07	0.128	0.128	0.142	0.128	0.142
	DDT	0.001	1.6	1.6	1.6	1.5	1.8
	α -cypermethrin	0.02	0.065	0.065	0.065	0.065	0.07
Winter	Fe	0.3	3.333	3.133	0.633	0.833	8.233
	Cu	2.0	0.065	0.105	0.1	0.08	0.1
	Zn	3.0	0.267	1.957	0.723	1.557	2.333
	Hg	0.006	0.12	0.117	0.12	0.125	0.132
	As	0.01	7.154	7.3	7.377	7.14	7.36
	Pb	0.01	4.954	4.867	4.9	4.86	5
	Cd	0.003	5.957	6.157	5.223	5.333	6.333
	Acetamiprid	0.07	0.128	0.117	0.114	0.128	0.135
	DDT	0.001	1.5	1.7	1.8	1.8	1.9
	α-cypermethrin	0.02	0.065	0.07	0.07	0.065	0.07

WHO: World Health Organization, DDT: Dichloro-diphenyl-trichloroethane, Hg: Mercury, As: Arsenic, Pb: Lead, Cd: Cadmium, Fe: Iron, Cu: Copper, Zn: Zinc

Overall, the HQ assessment underscores that arsenic, Cd, lead, and DDT are the dominant pollutants of concern in the LZR. The persistence of these contaminants highlights the need for stricter monitoring, effective pollution control measures, and targeted remediation strategies to mitigate both ecological and human health risks.

IV. CONCLUSION

The findings emphasize that precise selection of sampling points and timing is crucial for accurately capturing the chemical and environmental dynamics of the LZR. The physicochemical, heavy metals, and pesticides analysis of the LZR reveals clear seasonal and spatial variations in key water quality parameters, driven by natural factors and human activities, highlighting the influence of agricultural runoff, wastewater discharge, and climatic conditions on the river's chemical dynamics. Heavy metal concentrations exhibited both seasonal and spatial variability. For example, iron levels peaked at SP5 in winter (2.47 mg/L), while Cd levels reached their highest values at SP5 in autumn (0.027 mg/L). Similarly, arsenic and lead concentrations consistently showed the highest values at SP5 across all seasons, suggesting that this downstream site is more impacted by cumulative pollution from agricultural runoff and other anthropogenic sources. These patterns underscore the necessity for site-specific and seasonal monitoring to effectively control heavy metal and pesticide pollution in the region. To achieve this, targeted management strategies should be adopted, including stricter regulation and monitoring of agricultural inputs, enhancement of wastewater treatment facilities, implementation of riparian buffer zones to intercept runoff, and optimized sediment management at the dam to reduce the release of accumulated contaminants.

V. ACKNOWLEDGMENTS

The author would like to express sincere gratitude to the Department of Chemistry, Isfahan University of Technology, for providing the necessary resources and facilities that supported this work. Special thanks are also extended to Asst. Prof. Dr. Rawaz Rostam Hamadamin, Department of Geography, Faculty of Education, Koya University, Koya KOY45, Kurdistan Region – F.R. Iraq, for his valuable assistance. The author is further grateful to Dr. Jawameer Hama, Tenure Track Assistant Professor, Department of Agroecology, Aarhus University, Forsøgsvej 1, 4200 Slagelse, Denmark, for his continuous support and contributions.

REFERENCES

Afzal, W., Habib, S.S., Ujan, J.A., Mohany, M., and Bibi, H., 2024. Assessment of pesticide residues: A comprehensive analysis of seasonal trends and health implications. *Journal of Environmental Science and Health, Part B*, 59, pp.642-653.

Al-Barwary, M.R.A., Meshabaz, R.A., Hussein, N.J., and Ali, N.H., 2018. A comparison of water quality between well and spring samples selected from Soran District, Northern Erbil Governorate, Kurdistan Region - Iraq. *IOP Conference Series: Materials Science and Engineering*, 454, p.012062.

Al-Dabbas, M., 2024. Water resources of Iraq: An Overview. Springer, Cham, pp.49-81.

Altenburger, R., Brack, W., Burgess, R.M., Busch, W., Escher, B.I., Focks, A., Mark Hewitt, L., Jacobsen, B.N., de Alda, M.L., Ait-Aissa, S., Backhaus, T., Ginebreda, A., Hilscherová, K., Hollender, J., Hollert, H., Neale, P.A., Schulze, T., Schymanski, E.L., Teodorovic, I., Tindall, A.J., de Aragão Umbuzeiro, G., Vrana, B., Zonja, B., and Krauss, M., 2019. Future water quality monitoring: Improving the balance between exposure and toxicity assessments of real-world pollutant mixtures. *Environmental Sciences Europe*, 31, p.12.

American Public Health Association, 2017. Standard Methods for the Examination of Water and Wastewater. The Water Environment Federation. 23rd ed. American Public Health Association, United States.

ARO p-ISSN: 2410-9355, e-ISSN: 2307-549X

Carvalho, F.P., 2017. Pesticides, environment, and food safety. *Food Energy Security*, 6, pp.48-60.

Cayan, D.R., and Peterson, D.H., 1993. Spring climate and salinity in the San Francisco Bay Estuary. *Water Resources Research*, 29, pp.293-303.

Das, S., 2023. An Introduction to Water Quality Science, An Introduction to Water Quality Science. Springer International Publishing, Cham.

Ding, J., Zhao, P., Su, J., Dong, Q., Du, X., Zhang, Y., 2019. Aerosol pH and its driving factors in Beijing. *Atmos. Chem. Phys.*, 19, pp.7939-7954.

Hamadamin, R., Salih, M., and Hamad, N., 2018. Koya River Water Quality Assessment with a Focus on Physiochemical Properties and Heavy Metals. In: 2018 *International Conference on Pure and Applied Science*. Koya University, pp.206-212.

Hines, M.E., Berry Lyons, W., Armstrong, P.B., Orem, W.H., Spencer, M.J., Gaudette, H.E., and Jones, G.E., 1984. Seasonal metal remobilization in the sediments of Great Bay, New Hampshire. *Marine Chemistry*, 15, pp.173-187.

Hofmann, A.F., Middelburg, J.J., Soetaert, K., and Meysman, F.J.R., 2009. pH modelling in aquatic systems with time-variable acid-base dissociation constants applied to the turbid, tidal Scheldt estuary. *Biogeosciences*, 6, pp.1539-1561.

Jayaraj, R., Megha, P., and Sreedev, P., 2016. Organochlorine pesticides, their toxic effects on living organisms and their fate in the environment. *Interdisciplinary Toxicology*, 9, pp.90-100.

Kareem, A.T., Hamadamin, R.R., Mustafa, O., Karim, H.A., and Salih, M.Q., 2020. Transport modeling and leaching kinetics in groundwater of shiwashok oil field, Kurdistan Region, Iraq. *Tikrit Journal of Pure Science*, 25, pp.59-68.

Katimba, H.A., Wang, R., Cheng, C., Zhang, Y., Lu, W., and Ma, Y., 2024. Zinc absorption homeostasis in the human body: A general overview. *Food Reviews International*, 40, pp.715-739.

Kaur, R., Garkal, A., Sarode, L., Bangar, P., Mehta, T., Singh, D.P., and Rawal, R., 2024. Understanding arsenic toxicity: Implications for environmental exposure and human health. *The Journal of Hazardous Materials*, 5, p.100090.

Koh, D., Locke, S.J., Chen, Y., Purdue, M.P., and Friesen, M.C., 2015. Lead exposure in US worksites: A literature review and development of an occupational lead exposure database from the published literature. *American Journal of Industrial Medicine*, 58, pp.605-616.

Kumar, S., Rahman, M.A., Islam, M.R., Hashem, M.A., and Rahman, M.M., 2022. Lead and other elements-based pollution in soil, crops and water near a lead-acid battery recycling factory in Bangladesh. *Chemosphere*, 290, 133288.

Kumar, V., Pandita, S., Singh Sidhu, G.P., Sharma, A., Khanna, K., Kaur, P., Bali, A.S., and Setia, R., 2021. Copper bioavailability, uptake, toxicity and tolerance in plants: A comprehensive review. *Chemosphere*, 262, p.127810.

Lalín-Pousa, V., Conde-Cid, M., Díaz-Raviña, M., Arias-Estévez, M., and Fernández-Calviño, D., 2025. Acetamiprid retention in agricultural acid soils: Experimental data and prediction. *Environmental Research*, 268, p.120835.

Lazarević-Pašti, T., Anićijević, V., Baljozović, M., Anićijević, D.V., Gutić, S., Vasić, V., Skorodumova, N.V., and Pašti, I.A., 2018. The impact of the structure of graphene-based materials on the removal of organophosphorus pesticides from water. *Environmental Science: Nano*, 5, pp.1482-1494.

Li, D., Zou, M., and Jiang, L., 2022. Dissolved oxygen control strategies for water treatment: A review. *Water Science and Technology*, 86, pp.1444-1466.

Lu, Y., Chen, J., Xu, Q., Han, Z., Peart, M., Ng, C.N., Lee, F.Y.S., Hau, B.C.H., and Law, W.W.Y., 2023. Spatiotemporal variations of river water turbidity in responding to rainstorm-streamflow processes and farming activities in a mountainous catchment, Lai Chi Wo, Hong Kong, China. *Science of the Total Environment*, 863, p.160759.

Madhav, S., Ahamad, A., Singh, A.K., Kushawaha, J., Chauhan, J.S., Sharma, S., and Singh, P., 2020. *Water Pollutants: Sources and Impact on the Environment and Human Health*. Springer, Berlin. pp.43-62.

Marcheva, Z., Matev, S., Krenchev, D., and Simeonova, B., 2024. Seasonal variation of dissolved oxygen in river water in an urbanized area: example of the Vladayska River. *Review of the Bulgarian Geological Society*, 85, pp.79-87.

Martyniuk, C.J., Mehinto, A.C., and Denslow, N.D., 2020. Organochlorine pesticides: Agrochemicals with potent endocrine-disrupting properties in fish. *Molecular and Cellular Endocrinology*, 507, p.110764.

Mermer, S., Yalcin, M., and Turgut, C., 2020. The uptake modeling of DDT and its degradation products (o,p'-DDE and p,p'-DDE) from soil. *SN Applied Sciences*, 2, p.761.

Olsen, R.L., Chappell, R.W., and Loftis, J.C., 2012. Water quality sample collection, data treatment and results presentation for principal components analysis - literature review and Illinois River watershed case study. *Water Research*, 46, pp.3110-3122.

Park, J.S., Oh, S., Shin, M.Y., Kim, M.K., Yi, S.M., and Zoh, K.D., 2008. Seasonal variation in dissolved gaseous mercury and total mercury concentrations in Juam Reservoir, Korea. *Environmental Pollution*, 154, pp.12-20.

Peluso, J., Pérez Coll, C.S., Cristos, D., Rojas, D.E., and Aronzon, C.M., 2021. Comprehensive assessment of water quality through different approaches: Physicochemical and ecotoxicological parameters. *Science of the Total Environment*, 800, p.149510.

Pokhrel, G., and Rijal, M.L., 2020. Seasonal variation of springwater in-situ parameters in the bhusundi catchment, Gorkha, Nepal. *The Journal of Integrated Science and Technology*, 25, pp.45-51.

Prieto-Amparán, J.A., Rocha-Gutiérrez, B.A., Ballinas-Casarrubias, M. de L., Valles-Aragón, M.C., Peralta-Pérez, M.R., and Pinedo-Alvarez, A., 2018. Multivariate and spatial analysis of physicochemical parameters in an irrigation District, Chihuahua, Mexico. *Water*, 10, p.1037.

Qasim, S., 2024. Agriculture in Iraq. Springer, Berlin. pp.117-143.

Rather, R.A., Ara, S., Sharma, S., Padder, S.A., Lone, F.A., Mir, S.A., Baba, Z.A., Ayoub, I.B., Mir, I.A., Bhat, T.A., and Baba, T.R., 2022. Seasonal changes and determination of heavy metal concentrations in Veshaw river of the Indian western Himalaya. *Frontiers in Environmental Chemistry*, 3, p.1018576.

Rawal, S., Jose, J.P., Singh, D., and Linda, A., 2024. Ensuring water security by reviving selected springs in Kangra region, Himachal Himalaya, India. *Water Science*, 38, pp.239-255.

Schoeters, G., Hond, E.D., Zuurbier, M., Naginiene, R., Van DenHazel, P., Stilianakis, N., Ronchetti, R., and Koppe, J.G., 2006. Cadmium and children: Exposure and health effects. *Acta Paediatrica*, 95, pp.50-54.

Schreiber, S.G., Schreiber, S., Tanna, R.N., Roberts, D.R., and Arciszewski, T.J., 2022. Statistical tools for water quality assessment and monitoring in river ecosystems - a scoping review and recommendations for data analysis. *Water Quality Research Journal*, 57, pp.40-57.

Schwarzenbach, R.P., Escher, B.I., Fenner, K., Hofstetter, T.B., Johnson, C.A., von Gunten, U., and Wehrli, B., 2006. The challenge of micropollutants in aquatic systems. *Science*, 313, pp.1072-1077.

Shirasuna, H., Fukushima, T., Matsushige, K., Imai, A., and Ozaki, N., 2006. Runoff and loads of nutrients and heavy metals from an urbanized area. *Water Science and Technology*, 53, pp.203-213.

Sun, Q., Ma, J., Rifai, N., Franco, O.H., Rexrode, K.M., and Hu, F.B., 2008. Excessive body iron stores are not associated with risk of coronary heart disease in women. *Journal of Nutrition*, 138, pp.2436-2441.

Syers, J.K., Mackay, A.D., Brown, M.W., and Currie, L.D., 1986. Chemical and physical characteristics of phosphate rock materials of varying reactivity. *Journal of the Science of Food and Agriculture*, 37, pp.1057-1064.

Thakur, A., and Devi, P., 2024. A comprehensive review on water quality monitoring devices: Materials advances, current status, and future perspective. *Critical Reviews in Analytical Chemistry*, 54, pp.193-218.

Therrien, J.D., Nicolaï, N., and Vanrolleghem, P.A., 2020. A critical review of the data pipeline: how wastewater system operation flows from data to intelligence. *Water Science and Technology*, 82, pp.2613-2634.

Turusov, V., Rakitsky, V., and Tomatis, L., 2002. Dichlorodiphenyltrichloroethane (DDT): Ubiquity, persistence, and risks. *Environmental Health Perspectives*, 110, pp.125-128.

Valko, M., Morris, H., and Cronin, M., 2005. Metals, toxicity and oxidative stress. *Current Medicinal Chemistry*, 12, pp.1161-1208.

Wu, J., 2020. Challenges for safe and healthy drinking water in China.

Current Environmental Health Reports, 7, pp.292-302.

Wu, X., Cobbina, S.J., Mao, G., Xu, H., Zhang, Z., and Yang, L., 2016. A review of toxicity and mechanisms of individual and mixtures of heavy metals in the environment. *Environmental Science and Pollution Research*, 23, pp.8244-8259.

Yao, H., Qian, X., Gao, H., Wang, Y., and Xia, B., 2014. Seasonal and spatial variations of heavy metals in two typical chinese rivers: Concentrations, environmental risks, and possible sources. *International Journal of Environmental Research Public Health*, 11, pp.11860-11878.

ARO p-ISSN: 2410-9355, e-ISSN: 2307-549X